JGSP **28** (2012) 59–66

JOURNAL OF
Geometry and Symmetry in Physics
ISSN 1312-5192

MINIMAL SURFACE WITH A CAVITY OF GIVEN PERIMETER

ALEX BENJAMIN, RISHON BENJAMIN AND PAVEL GRINFELD

Communicated by Gregory L. Naber

Abstract. We pose a variant of the classical minimum surface problem inspired by a simple experiment with soap films: to find the surface of least area containing a cavity of given perimeter. We show that the equilibrium surface is governed by a system of two equations one of which is the zero mean curvature condition. The other equation states that the curvature of the cavity's contour is constant and that its principal normal lies in the plane tangential to the surface. A gradient descent simulation confirms the analytical equilibrium conditions and yields configurations qualitatively consistent with experiment.

1. Introduction

Soap films have for centuries been a source of beautiful mathematical problems. The mathematical problem discussed here is a variant of the classical minimal surface problem: Given a curved contour Γ in three dimensions and a positive number L, find a surface of least area that spans Γ and contains a cavity of perimeter L.

This problem is inspired by the soap film experiment in which a curved wire loop is dipped in a soap solution. A closed loop thread is then placed inside the soap film and the film on the interior of the thread is punctured. The system then relaxes to the equilibrium configuration seen in Fig. 1.

Fluid film experiments, in which the film stays intact, can only expose the net *normal* effect of surface tension. In order to observe the influence of surface tension more directly, one must expose the edge of the fluid film and let it deform due to surface tension. The described experiment does just that and thereby gives greater insight into the pointwise nature of surface tension.

Thin films have long been at the center of attention for many theorists, experimentalists and engineers. In recent decades, the number of unexpected and unexplained phenomena has actually grown and this has been reflected in the volume of publications in leading scientific journals. There is little doubt that this trend will continue. Many new problems arise from cutting edge experiments enabled by modern tools such as high speed cameras. Remarkably, simple and inexpensive experiments

doi: 10.7546/jgsp-28-2012-59-66

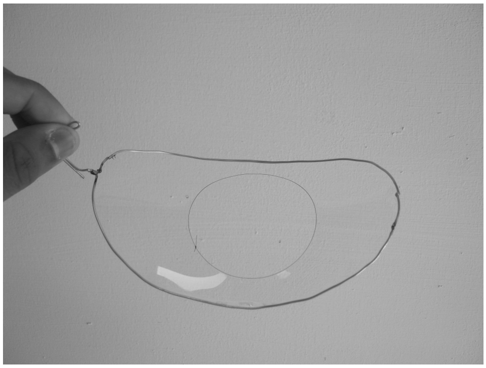

Figure 1. Equilibrium configuration. Equations (13) and (14) shows that the contour boundary has constant geodesic curvature k.

can also produce striking and novel effects. The experiment that gave rise to our problem was inspired by [1] and [15]. The possibility of simple experiments is a fortuitous circumstance given the remarkable importance of thin films and their unique physical properties. For classical reviews of fluid films see [6], [3].

Many aspects of fluid film behavior continue to be actively researched. Static and quasi-static effects include variation in thickness, concentration of surfactants. Foams and smectic films are receiving a great deal of attention [26]. Dynamic effects are significantly richer, and include changes in thickness [22], turbulence [16], [9], [24], [20], tremendous variations in thickness [9], [24], [22], [23] the Marangoni effect [25], draining and reverse draining [21], ejection of droplets [5], rupture [4], self-adaptation [2], and chaotic behavior [8]. It has been shown that surface tension can be controlled by the nanostructure properties of materials [7].

Fluid films also present an interface between two gases. When the volume of the surrounding gas is large, the inertia of the fluid film is not essential to the dynamics. These situations, where the film's main role is providing the force of surface tension, are relatively well understood and can be modeled realistically by modern numerical methods. When the mass of the fluid film is comparable to that of the ambient gas, as in the case of small soap bubbles, the inertia of the fluid film plays a major role. The authors of [17] report the break down of Rayleigh's classical formula (extended by Love to include the effect of the surrounding gas [18, pp 473-475]) for the oscillation of liquid drops under the influence of surface tension. Novel theoretical modeling is required to capture these effects.

Surface tension still remains to be one of the most intriguing classical forces. Under Laplace's model, in which the total energy is proportional to the surface area of the fluid film, the force of the surface tension acts in the plane tangential to the surface of the fluid film. Yet the net force acting upon a small patch points in the normal direction. For a *static*, but not necessarily equilibrium, fluid film, this follows from the formula

$$\int_\Gamma \mathbf{n}\ \mathrm{d}\Gamma = \int_S \kappa \mathbf{N}\,\mathrm{d}\,S \tag{1}$$

valid for any patch of the fluid film S with boundary Γ, where κ is mean curvature, $\mathbf{N}$ is the normal to the surface and $\mathbf{n}$ is the normal to the contour within the film's tangent plane as can be seen in Fig. 2.

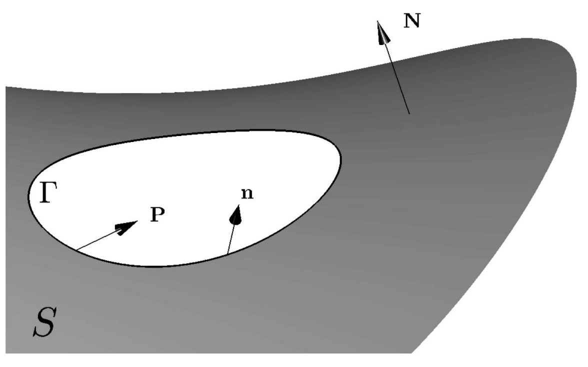

Figure 2. Geometric elements: $\mathbf{N}$ is the normal to the surface, $\mathbf{P}$ is the principal normal, $\mathbf{n}$ is the contour normal that lies within the tangent plane to the surface.

For a *moving* fluid film, the same conclusion follows from the recently formulated dynamic equations [10], [14]

$$\begin{aligned} \dot{\nabla}\rho + \nabla_\alpha\left(\rho V^\alpha\right) &= \rho C B^\alpha_\alpha \\ \rho\left(\dot{\nabla}C + 2V^\alpha \nabla_\alpha C + B_{\alpha\beta}V^\alpha V^\beta\right) &= -pB^\alpha_\alpha \\ \rho\left(\dot{\nabla}V^\alpha + V^\beta\nabla_\beta V^\alpha - C\nabla^\alpha C - CV^\beta B^\alpha_\beta\right) &= -\nabla^\alpha p \end{aligned} \tag{2}$$

where ρ is the two-dimensional density of the film (that is, in essence, its thickness), C and V^α are the normal and the tangential velocities of the fluid film, ∇_α is the covariant surface derivative, $\dot{\nabla}$ is the invariant time derivative [14] and p is the pressure associated with surface tension. The pressure p is negative since, given an elementary patch of the fluid film, the effect of surface tension is to pull it apart. The first equation in (2) is mass conservation, the second governs normal acceleration, while the third governs the tangential acceleration. Under Laplace's model of surface tension, p is constant

$$p = -\sigma \tag{3}$$

where σ is surface tension density. Therefore the right hand sides in equations (2) become $-\kappa\sigma/\rho$ and 0 respectively, indicating that the net surface tension force points in the normal direction.

The dynamic equations proposed in [10], [11] and extended in [12] to include viscosity and interaction with the ambient fluid, can be applied to more general models of surface tension that include arbitrary dependence on thickness as well as other parameters, such as curvature. An analysis of small oscillations of soap bubbles based on the dynamic equations proposed in [12] was given in [13] and included more general models of surface tension. The derived dispersion relationship can explain the discrepancy between the observed oscillation frequencies [17] and the Rayleigh's classical formula that ignores the inertia of the interface.

A deeper understanding of surface tension is all the more relevant since the Laplace model is insufficient in describing a number of fundamental effects associated with fluid films. Most notably, the Laplace model does not explain the variations in the thickness of the fluid film. For a *static* equilibrium fluid film configuration, the Laplace model implies $\kappa = 0$ but allows arbitrary distribution of thickness, inconsistent with everyday observations. For an *evolving* fluid film, the Laplace model does not provide a restoring force to a thickness disturbance and can therefore not explain the observed peristaltic density waves.

2. Equations of Equilibrium

Let $\tilde{\mathbf{V}}$ be the virtual velocities of the points along the cavity's boundary. Decompose

$$\tilde{\mathbf{V}} = \tilde{\mathbf{V}}_\Gamma + \tilde{\mathbf{V}}_P + \tilde{\mathbf{V}}_T \tag{4}$$

where $\tilde{\mathbf{V}}_\Gamma$ is the velocity along the boundary, $\tilde{\mathbf{V}}_P$ is the component along the principal normal $\mathbf{P}$ and $\tilde{\mathbf{V}}_T$ is the component along the torsion vector $\mathbf{T}$. Let C be the virtual velocity of the points on the surface in the direction of the normal $\mathbf{N}$. Then the variation δS of area S reads

$$\delta S = -\int_S C\kappa \,\mathrm{d}\, S + \int_\Gamma \left(\tilde{\mathbf{V}}_P + \tilde{\mathbf{V}}_T\right) \cdot \mathbf{n} \;\mathrm{d}\,\Gamma \tag{5}$$

where κ is the mean curvature of the surface.

Let $\tilde{\kappa}$ denote the curvature of the cavity's boundary. The constant length constraints is characterized by the equation

$$\frac{\mathrm{d}\,\tilde{V}_\Gamma}{\mathrm{d}\,s} - \tilde{\kappa}\tilde{V}_P = 0 \tag{6}$$

where s is the contour's arc length. Thus, δS can be written as

$$\delta S = -\int_S C\kappa \,\mathrm{d}\,S + \int_\Gamma \left(\frac{1}{\tilde{\kappa}} \frac{\mathrm{d}\,\tilde{V}_\Gamma}{\mathrm{d}\,s} \mathbf{P} + \tilde{\mathbf{V}}_T \right) \cdot \mathbf{n}\ \mathrm{d}\,\Gamma. \tag{7}$$

An integration by parts yields

$$\delta S = -\int_S C\kappa \,\mathrm{d}\,S + \int_\Gamma \left(-\tilde{V}_\Gamma \frac{\mathrm{d}}{\mathrm{d}\,s} \left(\frac{\mathbf{P}\cdot\mathbf{n}}{\tilde{\kappa}} \right) + \tilde{\mathbf{V}}_T \cdot \mathbf{n} \right) \mathrm{d}\,\Gamma. \tag{8}$$

Therefore, the equilibrium is characterized by the three equations

$$\kappa = 0, \qquad \mathbf{T}\cdot\mathbf{n} = 0, \qquad \mathbf{P}\cdot\mathbf{n} = \lambda\tilde{\kappa} \tag{9}$$

where λ is a constant of integration. The first equation in (9) is the familiar condition of vanishing mean curvature. As shown in Figure 2, the remaining equations indicate that the principal curvature $\mathbf{P}$ is colinear with the tangent normal $\mathbf{n}$ and that the curvature $\tilde{\kappa}$ of the contour boundary is constant:

$$\mathbf{P} = \mathbf{n}, \qquad \tilde{\kappa} = \text{const} \tag{10}$$

From (10) we can infer a condition on the geodesic curvature k of the countour boundary. Note that the following equation is satisfied by a general minimal surface ($\kappa = 0$):

$$\tilde{\kappa}\mathbf{P} = (\mathbf{n}\cdot B\mathbf{n})\,\mathbf{N} + k\mathbf{n} \tag{11}$$

where B is the full curvature tensor of the surface (its trace is κ and therefore 0). The quantity $\tilde{\kappa}\mathbf{P}$ is known as the *curvature normal*. From equation (11) we conclude that along the contour boundary, the surface curvature tensor B satisfies

$$\mathbf{n}\cdot B\mathbf{n} = 0. \tag{12}$$

Furthermore, the geodesic curvature k is constant (and matches the contour's curvature $\tilde{\kappa}$)

$$k = \tilde{\kappa}. \tag{13}$$

In summary, equation (10), the highlight of our analysis, can be expressed by the single equation

$$\tilde{\kappa}\mathbf{P} = \alpha\mathbf{n} \tag{14}$$

where α is constant. In words, *the curvature normal* $\tilde{\kappa}\mathbf{P}$ *of the equilibrium contour boundary has constant length and lies within the tangent plane of the minimal surface*.

3. Numerical simulation

The equilibrium equation (14) is deeply nonlinear and unlikely to yield analytical solutions. On the other hand, stable equilibrium configurations can be discovered numerically by implementing a gradient descent scheme that preserves the perimeter of the cavity. We represented the surface by a triangulated mesh with 3920 nodes and 7580 elements. We initially tessellated a circle with a cavity of diameter of about one quarter of the circle. Subsequently, we deformed the boundary according to the equation $0.15\cos 2\theta$ which is consistent with the deformation in Figure 1. For the initial configuration we adopted the shape $0.15\left(x^2-y^2\right)$ which matches the boundary deformation and is relatively close to the minimal configuration. The results of the gradient descent scheme can be seen in Fig. 3.

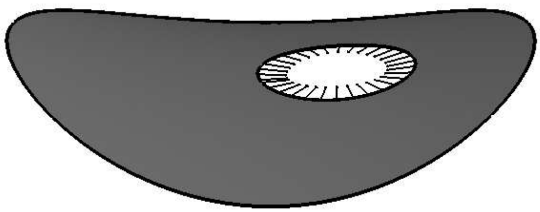

Figure 3. A gradient descent simulation of the equilibrium configuration. The figure illustrates the curvature normal field $\kappa\mathbf{P}$. It is evident that it is of constant magnitude and points along the tangent normal $\mathbf{n}$.

4. Conclusions

We have derived the governing equations for a minimal surface with a cavity of given perimeter. The necessary equations include the familiar zero mean curvature condition as well as a novel equation along the contour boundary of the cavity. The contour equation states that the curvature normal has constant length and is tangential to the surface. The outstanding questions include the stability of the equilibrium configuration and the extension of the equilibrium contour conditions to dynamics.

We would like to conclude with an important technical point. Our analysis assumed that the shape of the contour boundary is smooth. This assumption is consistent with the experimental observation but it is not always compatible with analysis based on the shape optimization approach. As was demonstrated in monograph [19], the boundary of the optimal shape is often not smooth but fractal. This aspect undoubtedly deserves further analysis.

References

[1] Soap Film Loops, *Natural Sciences Lecture Demonstrations*, Harvard University, Cambridge 2010.

[2] Boudaoud A., Couder Y. and Amar M., *Self-Adaptation in Vibrating Soap Films*, Phys. Rev. Lett. **82** (1999) 3847–3850.

[3] Boys B., *Soap Bubbles: Their Colors and Forces Which Mold Them*, Doubleday Anchor Books Garden City, New York 1959.

[4] Debregeas G., Martin P. and Brochard-Wyart F., *Viscous Bursting of Suspended Films*, Phys. Rev. Lett. **75** (1995) 3886–3889.

[5] Drenckhan M., Dollet B., Hutzler S. and Elias F., *Soap Films Under Large-Amplitude Oscillations*, Phil. Mag. Lett. **88** (2008) 669–677.

[6] Finn R., *Capillary Surface Interfaces*, Notices of the AMS **46** (1999) 770-781.

[7] Gerasopoulos K., McCarthy M., Banerjee P., Fan X., Culver J. and Ghodssi R., *Biofabrication Methods for the Patterned Assembly and Synthesis of Viral Nanotemplates*, Nanotechnology **21** (2010) 1-11.

[8] Gilet T. and Bush J., *Chaotic Bouncing of a Droplet on a Soap Film*, Phys. Rev. Lett. **102** (2009) 14501-1-4.

[9] Greffier O., Amarouchene Y. and Kellay H., *Thickness Fluctuations in Turbulent Soap Films*, Phys. Rev. Lett. **88** (2002) 94–101.

[10] Grinfeld P., *Exact Nonlinear Equations for Fluid Films and Proper Adaptations of Conservation Theorems from Classical Hydrodynamics*, J. Geom. Symmetry Phys. **16** (2009) 1–21.

[11] Grinfeld P., *A Variable Thickness Model for Fluid Films Under Large Displacements*, Phys. Rev. Lett. **105** (2010) 137802-1-4.

[12] Grinfeld P., *Viscous Equations of Fluid film Dynamics*, Computers, Materials and Continua, **19** (2010) 239-253.

[13] Grinfeld P., *Small Oscillations of a Soap Bubble*, Stud. Appl. Math., Cambridge, **128** (2011) 30-39.

[14] Grinfeld P., *A Better Calculus of Moving Surfaces*, J. Geom. Symmetry Phys. **26** (2012) 61–69.

[15] Jacobsen J., *As Flat As Possible*, SIAM Review **49** (2007) 491–507.

[16] Kellay H. and Goldburg W., *Two-Dimensional Turbulence: A Review of Some Recent Experiments*, Rep. Prog. Phys. **65** (2002) 845–894.

[17] Kornek U., Miller F., Harth K., Hahn A., Ganesan S., Tobiska L. and Stannarius R., *Oscillations of Soap Bubbles*, New J. Phys. **12** (2010) 073031-1-4.

[18] Lamb H., *Hydrodynamics*, Dover Publications, New York 1993.

[19] Lurie K., *Applied Optimal Control Theory of Distributed Systems*, Plenum Press, New York 1993.

[20] Martin B., Wu X., Goldburg W. and Rutgers M., *Spectra of Decaying Turbulence in a Soap Film*, Phys. Rev. Lett. **80** (1998) 3964–3967.

[21] Moulton D. and Pelesko J., *Reverse Draining of a Magnetic Soap Film*, Phys. Rev. E **81** (2010) 046320-1-4.

[22] Nierop E., Scheid B. and Stone H., *On the Thickness of Soap Films*: *An Alternative to Frankel's Law*, J. Fluid Mech **602** (2008) 119–127.

[23] Oprea J., *The Mathematics of Soap Films*: *Explorations with Maple*, American Mathematical Society, Providence 2000.

[24] Rivera M., Vorobieff P. and Ecke R., *Turbulence in Flowing Soap Films*: *Velocity, Vorticity, and Thickness Fields*, Phys. Rev. Lett. **81** (1998) 1417–1420.

[25] Tran T., Chakraborty P., Gioia G., Steers S. and Goldburg W., *Marangoni Shocks in Unobstructed Soap-Film Flows*, Phys. Rev. Lett. **103** (2009) 104501.

[26] Trittel T., Aldred R. and Stannarius R., *Plateau Borders of Smectic Liquid Crystalline Films*, Phil. Mag. **91** (2011) 2343–2354.

Alex Benjamin
Mechanical Engineering
Drexel University
USA
E-mail address: `arb93@drexel.edu`

Rishon Benjamin
Chemical Engineering
Drexel University
USA
E-mail address: `rrb67@drexel.edu`

Pavel Grinfeld
Department of Mathematics
Drexel University
Philadelphia, PA 19105
USA
E-mail address: `pg@freeboundaries.com`